Organic & Biomolecular Chemistry

Accepted Manuscript

ROYAL SOCIETY OF CHEMISTRY

www.rsc.org/obc

Triazolopyridopyrimidines: an emerging family of effective DNA photocleavers. DNA binding. Antileishmanial activity†

Rosa Adam,[a] Pablo Bilbao-Ramos,[b] Belén Abarca,[*a] Rafael Ballesteros,[*a] M. Eugenia González-Rosende,[c] M. Auxiliadora Dea-Ayuela,[b,c] Francisco Estevan,[d] Gloria Alzuet-Piña[*e]

[a]*Departament de Química Orgànica, Facultat de Farmàcia, Universitat de València, Av. Vicent Andrés Estellés s/n, 46100 Burjassot (Valencia), Spain*

E-mail: Rafael.Ballesteros@uv.es, Belen.Abarca@uv.es

[b]*Departamento de Parasitología, Universidad Complutense de Madrid, Plaza Ramón y Cajal s/n, 28040 Madrid, Spain*

[c]*Departamento de Farmacia, Universidad CEU Cardenal Herrera, Avda. Seminario s/n, 46113 Moncada (Valencia), Spain*

[d]*Departament de Química Inorgànica, Facultat de Química, Universitat de València, Dr. Moliner 50, 46100 Burjassot (Valencia), Spain*

[e]*Departament de Química Inorgànica, Facultat de Farmàcia, Universitat de València, Av. Vicent Andrés Estellés s/n, 46100 Burjassot (Valencia), Spain*

E-mail: Gloria.Alzuet@uv.es

†Electronic supplementary information (ESI) available.

Abstract

Triazolopyridopyrimidines 3-phenyl-6,8-di(2-pyridyl)-[1,2,3]triazolo[5',1':6,1]pyrido[2,3-*d*]pyrimidine (**1a**), 6,8-di(pyridin-2-yl)-[1,2,3]triazolo[1',5':1,6]pyrido[2,3-*d*]pyrimidine (**1b**) and 3-methyl-6,8-di(2-pyridyl)-[1,2,3]triazolo[5',1':6,1]pyrido[2,3-*d*]pyrimidine (**1c**) were prepared and their electrochemical and luminescent properties were deeply studied. The DNA binding ability of this series of compounds has been investigated by means of UV-vis absorption and fluorescence titrations, steady-state emission quenching with ferrocyanide as well as viscosity measurements. Results have shown that triazolopyridopyrimidine **1a** interacts strongly at DNA grooves. This compound also displays preferential binding to GC-rich sequences and ability to photooxidize guanine. Moreover, these studies have revealed the key role of the phenyl substituent at the triazole ring in the binding affinity of **1a-c**. Compounds **1b** and **1c** did not show appreciable propensity for DNA binding however, these triazolopyridopyrimidines demonstrated to present photoinduced DNA cleavage activity being **1b** more active than **1c**. DNA photocleavage mediated by these compounds takes place mainly through single strand scission events and, in a minor extent, through double strand cuts. Mechanistic investigations using radical scavengers showed that both **1b** and **1c** generate reactive oxygen species (singlet oxygen, superoxide and hydroxyl radicals) upon irradiation. Both type I and type II mechanisms are involved in the photocleavage process. Furthermore, compounds **1a-c** were tested for their antiprotozoal activity against four different *Leishmania* spp. (*L. infantum*, *L. braziliensis*, *L. guyanensis* and *L. amazonensis*). Triazolopyridopyrimidines **1a** and **1c** resulted to be more active and selective than the reference drug (miltefosine) *in vitro* against *L. infantum* amastigotes. Compound **1a** exhibited high leishmanicidal activity against *L. infantum* spleen forms in the *in vivo* test.

Introduction

Small molecules targeting DNA have attracted significant scientific interest due to their medicinal, biochemical and biological applications. The most common non-covalent interaction modes of such systems with DNA are intercalation and major or minor groove binding. Many therapeutic agents, particularly anticancer drugs, are known to bind DNA via these motifs. Moreover, the possibility of gene modulation by sequence specific binding of small molecules to DNA has also been explored.[1]

Nowadays, the design of DNA cleavage agents is one of the areas in which chemists have made substancial efforts and can provide significant contributions to antiprotozoal and antitumor chemotherapy.[2] Within this context, the development of synthetic nucleases that are activated upon irradiation has gained importance in the chemistry of photodynamic therapy (PDT). PDT has emerged as a clinical modality for the treatment of certain cancers, age related macular degeneration, psoriasis and other diseases. It requires a photosensitive drug, light of a specific wavelength and molecular oxygen to induce a series of photochemical reactions resulting in the formation of reactive oxygen species, mainly singlet oxygen, which is the major cytotoxic agent. The great advantages of this therapy are its non-invasive nature and its large selectivity that affords the selective irradiation, avoiding the important side effects of most cytotoxic drugs.[3]

1,2,3-Triazole compounds do not exist in natural substances but they have been widely investigated due to their attractive features, such as their large dipole moments, stability to metabolic degradation and capacity to form hydrogen bonds.[4] 1,2,3-Triazole derivatives have shown to present a great potential in medicinal chemistry. In the last years, several compounds containing 1,2,3-triazole scaffold, such as quinolone triazoles,[5] triazol naphtalimides[4] or triazoloacridones,[6] able to interact with DNA have been described. The anticancer activity of the latter family of compounds is remarkable,[7] in particular that of triazoloacridone C-1305, which is active against breast cancer,[8] colon cancer[9] and leukemia.[10] The antitumor activity of this compound was found to be due to its ability to inhibit topoisomerase II, a fact that could be directly related to its capacity for intercalating between DNA nucleobases. Moreover, molecules containing a triazole scaffold have also shown good activities against *Leishmania spp*.[11] Recently, we have reported the first [1,2,3]triazolo[1,5-*a*]pyridine compounds with leishmanicidal activity.[12] These novel compounds have also shown to be good DNA binders, in a similar way to that described for other antiprotozoal drugs active against Leishmaniasis, such as pentamidine[13] or furamidine.[14]

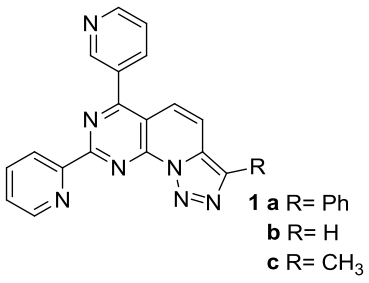

Figure 1. General structure of triazolopyridopyrimidines.

Supported by these promising results, we decided to explore the DNA binding potential and leishmanicidal activity of another compounds series containing the triazolopyridine scaffold but with a more extended π system that could enhance the DNA affinity of triazolopyridine compounds. We have selected the useful fluorescent anion sensors triazolopyridopyrimidines **1** (Figure 1)[15] whose structure, consisting of three fused heteroaromatic rings, suggests that they could be suitable DNA binders. Moreover, their luminescent properties encouraged us to study

the photo-induced DNA cleavage promoted by these compounds, as a part of our ongoing interest on the development of new antitumor agents.

In this work, the DNA binding properties of triazolopyridopyrimidines **1** (**1a-c**) were investigated in depth with both genomic duplex DNA and synthetic sequences. Also included are the results of the biological activity studies carried out to evaluate their ability to induce DNA photocleavage and to clarify the DNA scission process mechanism. Finally, the *in vitro* and *in vivo* antileishmanial activity of the compounds against several *Leishmania spp* was tested.

Results and discussion

Synthesis and characterization

Triazolopyridopyrimidine **1a** (3-phenyl-6,8-di(2-pyridyl)-[1,2,3]triazolo[5´,1´:6,1]pyrido[2,3-*d*]pyrimidine) was prepared in 36% yield by regioselective lithiation of the triazolopyridine **2a** with *n*-BuLi in toluene at -40 ºC, and subsequent reaction of the obtained 7-lithio triazolopyridine with 2.1 equivalents of 2-cianopyridine. The identity and purity of **1a** was confirmed by HRMS, ^{1}H and ^{13}C NMR (Figure S1).

Synthesis of triazolopyridopyrimidines **1b** and **1c** was achieved by using the same methodology, as previously described by our research group.[15a, b]

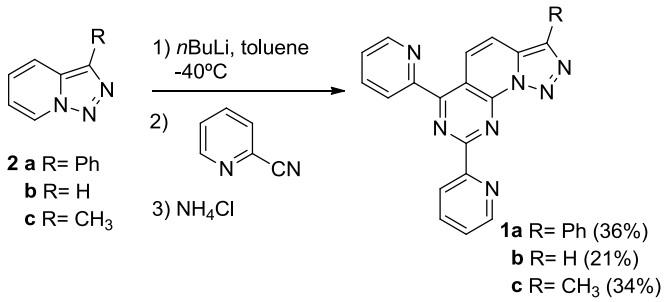

Scheme 1. Synthesis of triazolopyridopyrimidines **1a-c**.

It is known that both photophysical and electrochemical properties of the compounds are closely related to their biological activity and, in particular, to their ability to induce DNA photocleavage.[16] For this reason, we studied the photophysical and electrochemical properties of triazolopyridopyrimidines **1** as a first stage of our work.

Table 1. UV-vis and fluorescent data of compounds **1**.[a]

	UV λ_{max}/nm (log ε)	Fluorescence Emission λ_{max} /nm	Fluorescence Excitation λ_{max} /nm
1a	280 (4.21), 387 (3.95)	519	286, 376
1b	283 (4.31), 356 (4.14)	455	285, 360
1c	283 (4.24), 366 (4.01)	481	286, 368

[a]solvent: cacodylate buffer 0.1 M, pH= 6.0, 5% DMF.

The absorption and luminiscence spectra of compounds **1a-c** were recorded in the solvent used for the biological assays (cacodylate buffer 0.1 M, pH= 6.0, 5% DMF). Spectroscopic data

are summarized in Table 1. The three compounds display two well-defined absorption bands ascribed to π-π* transitions: an intense band at around 280 nm and another one, with lower intensity, centered between 356 and 387 nm. Notably, substitution has no effect on the maximum around 280 nm whereas the long-wavelength maximum depends significantly on the electron donating properties of the triazole ring substituent. The red-shifted absorption maximum in **1a** and **1c** as compared with **1b** is in good agreement with the electron-donating effect of phenyl and, in minor extent, of methyl groups.[17] The fluorescence emission maximum of the compounds follow the same order: λ_{max} (**1a**) > λ_{max} (**1c**) > λ_{max} (**1b**). However, the electronic nature of the substituent at the triazole ring has a major effect on the position of the emission maximum than on that of the corresponding absorption band.

Electrochemical properties of triazolopyridopyrimidines **1** were studied by cyclic voltammetry. Cyclic voltammograms, registered from -0.7 V to -1.5 V, are shown in Figure 2 and electrochemical data are collected in Table 2.

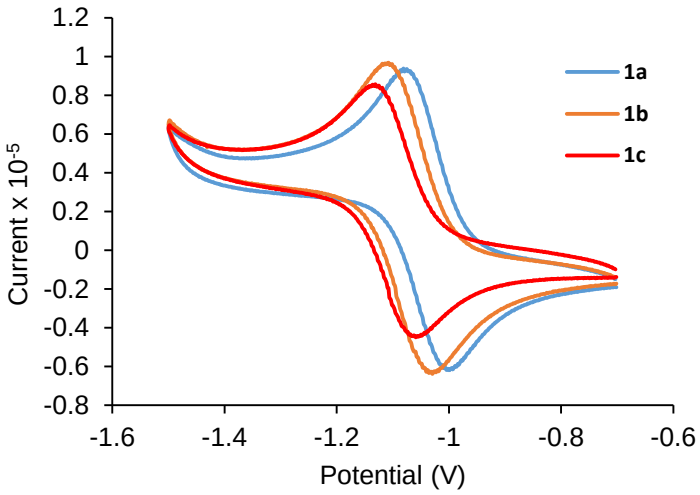

Figure 2. Cyclic voltammograms of triazolopyridopyrimidines **1** (2.5 mM) in DMF. **1a** (blue line), **1b** (orange line) and **1c** (red line). Scan rate 50 mV/s.

The formal reduction potential values ($E_{1/2}$), -1.04 V for **1a**, -1.07 V for **1b** and -1.09 V for **1c**, were determined averaging the potentials of the anodic (E_{pa}) and cathodic (E_{pc}) peaks. As can be appreciated, these potential values were dependent on the substituent at the triazole ring. In fact, **1a** exhibited the most oxidazing power which could be explained by the high stability of its reduced state because of major electron delocalization possibilities provided by the phenyl group. The lowest $E_{1/2}$ value for **1c** and, consequently, its less oxidizing power, could be due to the electron donor effect of methyl group that leads to a major destabilization of the triazolopyridopyrimidine reduced state.

Table 2. Electrochemical data of triazolopyridopyrimidines **1**.

	E_{pc} (V)	E_{pa} (V)	$E_{1/2}$ (V)	ΔE_p (mV)	$\lvert I_{pa}/I_{pc} \rvert$
1a	-1.08	-1.00	-1.04	-80	0.93
1b	-1.10	-1.03	-1.07	-70	0.95
1c	-1.13	-1.05	-1.09	-80	0.88

Interestingly, the three compounds undergo a reversible reduction process, as judged from their potential differences ($\Delta E_p = E_{pc} - E_{pa}$) and the ratios of anodic and cathodic peak currents ($|I_{pa}/I_{pc}|$) close to 1.[18]

DNA binding studies

DNA binding is the critical step for the study of effective chemotherapeutic agents and, in particular, antitumor drugs. The interaction of triazolopyridopyrimidines **1a-1c** with DNA was studied by means of absorption spectroscopy, fluorescence spectroscopy and viscosimetry.

UV-visible titrations

Complexation between a ligand and DNA leads to spectroscopic changes that can be used to monitor the binding process. Compounds solutions (20 μM) were titrated with CT-DNA (2–100 μM). As shown in Figure 3, the addition of CT DNA induced important changes in the characteristic absorption bands at 280 and 387 nm of compound **1a**. A significant hypochromism was observed from the first DNA addition ([DNA]/[**1a**]= 0.1) which reached *ca.* 40% at a DNA to **1a** molar ratio of 5. A moderate bathochromic effect ($\Delta\lambda$ = 5 nm) was also found in the band at 387 nm. Changes in the UV spectrum of **1a** upon DNA addition are clearly indicative of the interaction of **1a** with DNA. Furthemore, the isosbestic point at 430 nm reveals a one step equilibrium of two species in solution, **1a** and **1a**-DNA.[19] On the other hand, the extent of hypochromism and red-shifting shows a strong binding of compound **1a** to DNA[20] and could be a first evidence of a possible intercalation of **1a** between the base pairs of CT-DNA, although the exact binding mode cannot be merely proposed by UV-visible studies since different types of DNA interaction can induce qualitatively similar effects.[21]

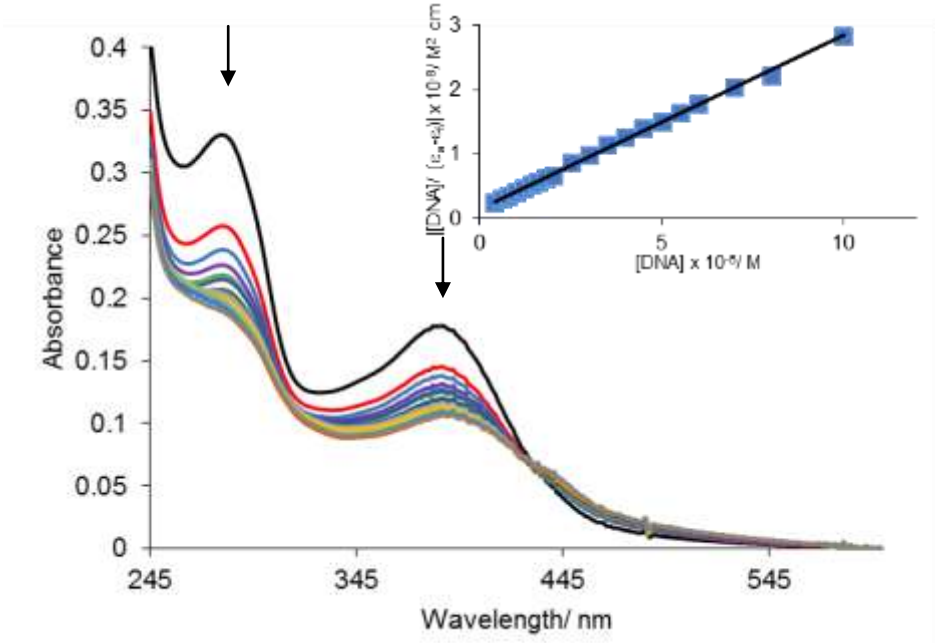

Figure 3. UV spectra of **1a** (20 μM) in cacodylate buffer 0.1 M, pH= 6.0, 5% DMF, in the absence (black line) and in the presence of increasing concentrations of CT-DNA (2- 100 μM). Arrows show the changes in absorbance with the increase in DNA concentration. Inset: plot of [DNA]/(ε_a- ε_f) versus [DNA].

In order to further evaluate quantitatively the DNA-binding affinity of **1a**, the intrinsic binding constant (K_b) was obtained by monitoring the changes in absorbance of the band at 387 nm using the following equation [1]:[22]

$$[DNA]/(\varepsilon_a - \varepsilon_f) = [DNA]/(\varepsilon_b - \varepsilon_f) + 1/[K_b\,(\varepsilon_b - \varepsilon_f)] \qquad [1]$$

where [DNA] is the concentration of DNA in nucleotides, $\varepsilon_a = A_{obsd}/[compound]$, ε_f is the extinction coefficient for the free compound and ε_b is the extinction coefficient for the compound in the fully DNA-bound form. In plots of $[DNA]/(\varepsilon_a - \varepsilon_f)$ versus [DNA], K_b is given by the ratio of the slope to the intercept.

The binding constant value of 7.8 x 10^4 M^{-1} for **1a** is similar to those calculated for triazol derivatives that presented a high DNA affinity and have been considered as DNA intercalators.[7, 23] Also, the magnitude of this binding constant is close to that found for related triazolopyridyl compounds that interact with DNA at grooves.[12] Therefore, based on the K_b value of **1a**, a groove or/and intercalative binding mode for this compound can be proposed.

UV absorption titrations of **1b** and **1c** with CT-DNA were also performed. Surprisingly, the UV spectra of these compounds displayed virtually no changes when DNA was added (Figure S2), suggesting that these compounds are not able to interact with DNA.

Luminiscence titrations

The fluorescence emission of drugs bound to DNA can be either enhanced, as observed for ethidium bromide,[24] or efficiently quenched, as found for certain aminoacridines and anthracyclines, including daunomycin[25] and adriamycin.[26] Triazolopyridopyrimidines **1a-1c** are fluorescent compounds so that, their DNA interaction was also studied by measuring the changes in their fluorescence emission in the presence of DNA.

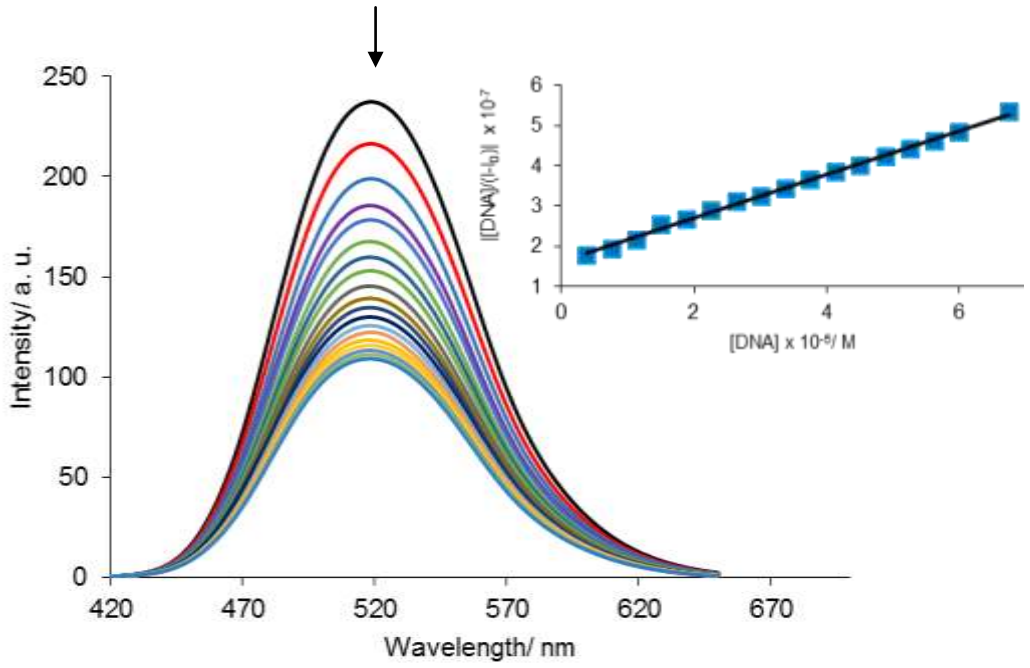

Figure 4. Fluorescence emission spectra of **1a** (15 μM) in cacodylate buffer 0.1 M, pH= 6.0, 5% DMF in the absence and the presence of increasing amounts of CT-DNA at concentrations ranging from 3.75 to 75 μM. Arrow indicates the effect of CT-DNA in the fluorescence emission of the compound. Inset: plot of $[DNA]/(I - I_0)$ versus [DNA].

Fluorescence emission titration was first carried out with **1a**, compound that, as shown above, has provided positive results in UV titration studies. The emission of **1a** fluorescence was measured using an excitation wavelength of 376 nm in the presence of increasing amounts of CT-DNA (Figure 4). The fluorescence of **1a** (λ_{max} = 519 nm) was efficiently quenched upon the addition of DNA. The remarkable decrease in fluorescence intensity clearly indicates a strong interaction of **1a** with DNA and also confirms the results obtained from absorption titration.

The intrinsic binding constant (K_b) was obtained using equation [2] that has been adapted by us from equation [1]:

$$[DNA]/(I- I_0)= [DNA]/ (I_b- I_0) + 1/[K_b (I_b – I_0)] \quad [2]$$

where [DNA] is the DNA concentration in nucleotides, I is the maximum emission intensity measured for each addittion, I_0 is the maximum emission intensity for the free compound and I_b is the maximum fluorescence emission for the compound in the fully DNA-bound form.

The K_b value of 6.9 x 10^4 M^{-1} is in very good agreement with the one calculated from UV absorption titration. Moreover, this value is similar to those calculated by this method for small organic molecules that interact strongly with DNA.[1, 27]

Similarly, fluorescence titrations were carried out with compounds **1b** and **1c** (Figure S3). **1b** and **1c** showed no significant changes in their fluorescence emission upon DNA addition, a fact that could be expected considering the above described results for UV titration.

DNA-induced luminescent quenching is a well-studied phenomenon.[27] Usually, this effect indicates the quenching of the excited state through photooxidation processes that involve nucleobases, commonly G sites.[27-28] This is the case of some small organic molecules that were found to interact with DNA such as coumarines[29] and dipyridophenazine (dppz).[27]

In this context, we considered that the analysis of the possible nucleosides oxidation by our compounds could be of interest. Seidel *et al.*[29] determined the reduction potencials of nucleosides in DMF and they obtained values of: <-2.76 V for guanosine, -2.52 V for adenosine, -2.35 V for cytidine and -2.18 V for thymidine. From these potential values it is clear that our compounds, with reduction potentials between -1.04 V to -1.09 V, are sufficiently reactive to oxidize the four nucleosides being oxidation of guanosine the most favorable process. This reaction, therefore, could be considered feasible for our three compounds. However, emission intensity quenching was only detected for compound **1a**, a fact that could be explained taking into account that **1a** is the only compound able to interact with DNA.

Steady-state emission quenching experiments using $[Fe(CN)_6]^{4-}$ as quencher were also performed since they may provide a better understanding of the interaction of **1a** with DNA. A highly negatively charged quencher is expected to be repelled by the negatively charge phosphate backbone of DNA and, therefore, a more deeply DNA-bound compound should be more protected from quenching than a loosely or shallowly bound ligand.[30] Luminiscence quenching of molecules bound to DNA by ferrocyanide has often used to assign the DNA binding mode as intercalation. However, Turro *et al.* have recently demonstrated that the absence of quenching by $[Fe(CN)_6]^{4-}$ cannot be considered a proof of an intercalation binding mode, but it suggests a strong interaction of the compound with the DNA.[31]

As illustrated in Figures S4a and S4b, in the absence of DNA an important quenching of **1a** fluorescence emission was observed with increasing amounts of $[Fe(CN)_6]^{4-}$, while in the presence of CT-DNA **1a** fluorescence was poorly quenched by $[Fe(CN)_6]^{4-}$.

The quenching efficiency was evaluated by the Stern-Volmer constant (K_{SV}) calculated from equation [3]:

$$I_0/I = 1 + K_{SV} [K_4[Fe(CN)_6]] \quad [3]$$

where I is the maximum intensity of **1a** fluorescence emission for each addition of $K_4[Fe(CN)_6]$, I_0 is the maximum intensity of **1a** fluorescence emission in the absence of $K_4[Fe(CN)_6]$, $[K_4[Fe(CN)_6]]$ is the concentration of the quencher and K_{SV} is the Stern-Volmer constant.

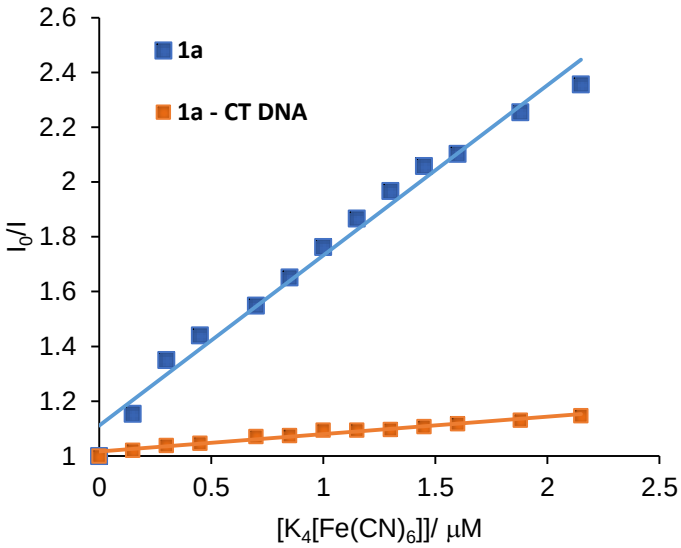

Figure 5. Stern-Volmer plot of **1a** fluorescence titration with $[K_4Fe(CN)_6]$ in the absence of CT-DNA (blue) and in the presence of CT-DNA (orange).

Stern-Volmer plots for both experiments, in the absence and the presence of DNA, are represented in Figure 5. The K_{SV} value of **1a** in the absence of DNA was 6.25 x 10^5 M^{-1}, while in the presence of DNA the constant value was decreased to 6.38 x 10^4 M^{-1}. This remarkable difference in the quenching efficiency would be justified by a strong interaction of **1a** with DNA, since such interaction protects the compound from the accessibility of $[Fe(CN)_6]^{4-}$ being in that way quenched to a lesser extent.

To get a better insight into **1a** binding to DNA, we explored its potential base-specific nucleotide binding. With this aim, fluorescence titrations with synthetic alternating copolymers of adenine-thymine, poly(dA-dT)$_2$, and guanine-cytosine, poly(dG-dC)$_2$, were carried out (Figure 6).

The emission-spectral response of **1a** on addition of polynucleotides is similar to that observed with CT-DNA. A large decrease in emission intensity was found for both poly(dA-dT)$_2$ and poly(dG-dC)$_2$. The intrinsic binding constants, calculated by means of equation [2], were 5.6 x 10^4 M^{-1} and 1.9 x 10^5 M^{-1} for poly(dA-dT)$_2$ and poly(dG-dC)$_2$, respectively. Interestingly, a comparison of the binding constants reveals that **1a** presents a similar affinity for CT-DNA (K_b = 6.9 x 10^4 M^{-1}) and poly(dA-dT)$_2$. However, the slightly higher binding affinity for poly(dG-dC)$_2$ showed by **1a** suggests that it exhibits some preference for the GC.CG step sequence.[27, 28b]

Viscosimetry measurements

Photophysical proofs provide necessary but not sufficient clues to support a DNA binding mode. Hydrodynamic measurements that are sensitive to length changes are regarded as the least ambiguous and the most critical tests of a DNA binding model in solution, providing reliable evidence for the DNA binding mode. One classic intercalation model results in the lengthening of the DNA helix as the base pairs are separated to accommodate the binding molecule, thus leading to an increase in DNA viscosity. In contrast, compounds that bind exclusively in DNA grooves by means of partial and/or nonclassical intercalation typically

cause either a less pronounced (positive or negative) change or no change at all in DNA solution viscosity.[32] The binding mode of compound **1a** to DNA was elucidated from viscosity measurements. In these studies, viscosities of a CT-DNA solution (η_0) and a CT-DNA solution with different amounts of the tested compound (η) were measured.

Results (Figure S5) show that this compound does not cause important changes in DNA solution viscosity. Therefore, **1a** intercalation between DNA base pairs could be ruled out.

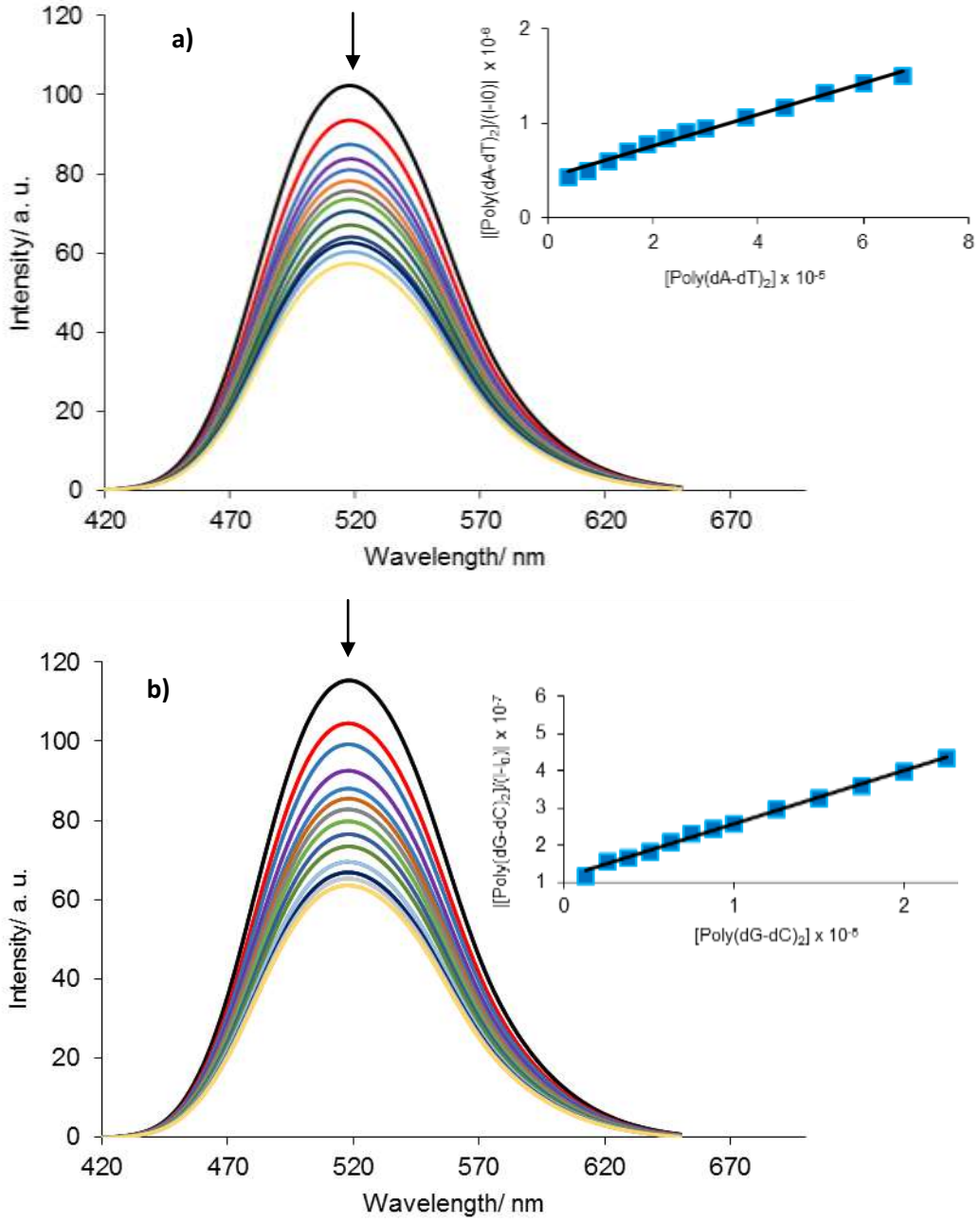

Figure 6. a) Fluorescence emission spectra of 15 μM **1a** in cacodylate buffer 0.1 M, pH= 6.0, 5% DMF in the absence and in the presence of increasing amounts of poly(dA-dT)$_2$ [3.75-67.5 μM]. Inset: plot of [poly(dA-dT)$_2$]/(I- I$_0$) versus [poly(dA-dT)$_2$]. **b)** Fluorescence emission spectra of 5 μM **1a** in cacodylate buffer 0.1 M, pH= 6.0, 5% DMF in the absence and in the presence of increasing amounts of poly(dG-dC)$_2$ [1.25-22.5 μM]. Arrows indicate the effect of DNA in fluorescence emission. Inset: plot of [poly(dG-dC)$_2$]/(I- I$_0$) versus [poly(dG-dC)$_2$].

The binding studies collectively show that **1a** interacts with DNA in the grooves or in the sugar–phosphate backbone. Taking into account the structural differences within this series of compounds, a **1a**-DNA binding driven mainly by hydrophobic interactions involving the benzene ring can be clearly proposed. Moreover, compound **1a** would be able to form hydrogen bonds with the nucleobases and/or the sugar phosphate backbone acting as an acceptor through its pyridine and triazolopyrimidine nitrogen atoms.

In order to confirm the results derived from UV and fluorescence spectroscopy and with the aim to discard that compounds **1b** and **1c** could interact weakly with DNA without modifying significantly their optical properties, viscosity measurements with **1b** and **1c** were also performed. As could be expected, both compounds did not modify DNA viscosity (Figure S5) which, in addition, supports the fact that the benzene ring at triazolopyrimidine system has an important role on the propensity for DNA binding of this series of compounds.

DNA photocleavage

Triazolopyridopyrimidines **1** have shown to be redox active and light sensitive compounds. Therefore, triazolopyridopyrimidines **1** could be attractive molecules for being used as photosensitizers in photodynamic therapy (PDT). In general, photoactivation of PDT drugs in the presence of oxygen results in the formation of reactive species, mainly singlet oxygen, but also superoxide or hydroxyl radicals. These reactive species can cause oxidative damage to biomolecules, including nucleic acids.[33] In this regard, we have tested the potential DNA photocleavage activity of triazolopyridopyrimidines **1**. As shown previously, **1a** is the only compound able to interact with DNA but, as DNA binding is not a necessary condition for a DNA photocleaver,[34] the DNA cleavage ability for the three compounds **1a-c** was evaluated. In addition, compounds **1b** and **1c** present better solubility in aqueous media than compound **1a**.

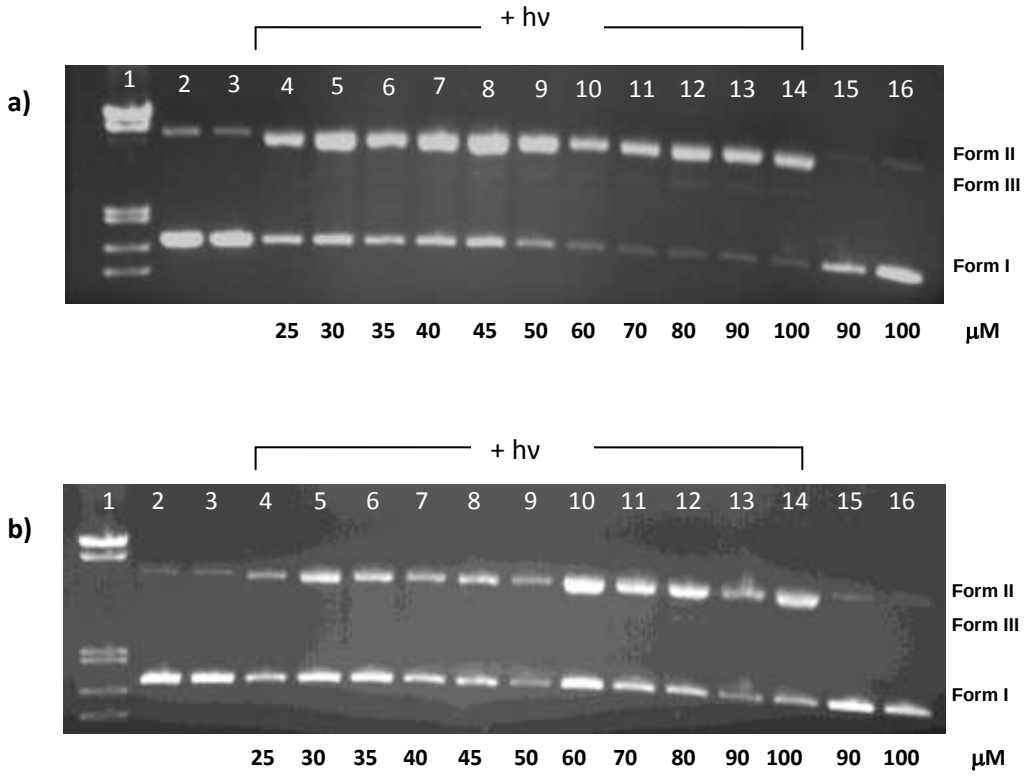

Figure 7. Agarose gel electrophoresis of pUC18 in the presence of compounds **1b** (a) and **1c** (b) upon photo-irradiation at 365 nm for 2 h. 1: λDNA/EcoR1+HindIII Marker; 2: DNA control without irradiation; 3: DNA control; 4: compound 25 µM ; 5: compound 30 µM; 6: compound 35 µM; 7: compound 40 µM; 8: compound 45 µM; 9: compound 50 µM; 10: compound 60 µM;

11: compound 70 μM; 12: compound 80 μM; 13: compound 90 μM; 14: compound 100 μM; 15: compound 90 μM without irradiation ; 16: compound 100 μM without irradiation.

The photoinduced cleavage of SC pUC18 DNA by triazolopyridopyrimidines **1** was studied upon irradiation with UV-A light at 365 nm. The extent of cleavage was monitored by agarose gel electrophoresis. When plasmid DNA is subjected to electrophoresis, the fastest migration will be observed for the intact supercoiled form (Form I). If scission occurs on one strand (nicking), the supercoils will relax to generate a slower moving open circular form (Form II). If both strands are cleaved, a linear form (Form III) that migrates between Forms I and II will be generated.

Firstly, the photocleavage ability of compound **1a** was explored. Due to the poor solubility of this compound in aqueous media only low concentrations from 5 to 18 μM could be assayed. Surprisingly, although this compound has shown to interact strongly with DNA, triazolopyridopyrimidine **1a** resulted unable to mediate DNA photocleavage (Figure S6). No open circular DNA (Form II) or linear DNA (Form III) were detected for all the concentrations at the assayed conditions (compare lane 3 with lanes 4-9, Figure S6).

Contrary to that observed for **1a**, compounds **1b** and **1c** can promote DNA cleavage upon irradiation (Figure 7). In particular, **1b** at concentrations between 25 and 60 μM (lanes 4-10, Figure 7a) was able to partially transform supercoiled DNA (Form I) into open circular DNA (Form II) and to a much lesser (negligible) extent to linear DNA (Form III). At concentrations higher than 60 μM (lanes 11-14, Figure 7a), no difference in photocleavage was observed indicating a saturation of photocleavage activity at this concentration. Compound **1c** was not able to promote the whole degradation of supercoiled DNA (Figure 7b) and open circular DNA (Form II) was detected for all the evaluated concentrations. A very small amount of linear DNA (Form III) was only obtained for the highest concentrations (60-100 μM) (lanes 10-14, Figure 7b). Quantitative data, collected in Figure 8 and Tables S1 and S2, clearly show that both compounds behave as DNA photocleavers being **1b** a more efficient photonuclease than **1c**.

Control experiments with both compounds without irradiation (lanes 15 and 16, Figure 7a and 7b) failed to show DNA cleavage indicating that, primarily, the excited states of triazolopyridopyrimidines **1b** and **1c** are responsible for the DNA cleavage.

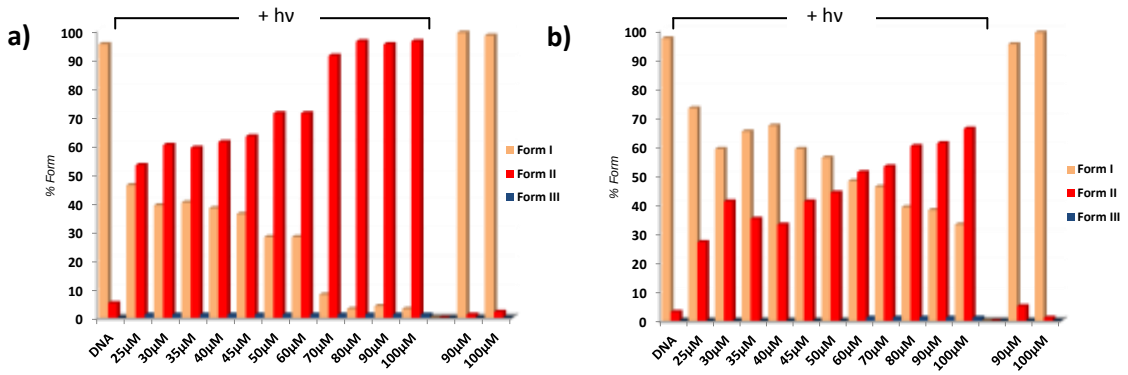

Figure 8. Bar diagram representing relative amounts of the three forms of plasmid DNA after irradiation in the presence of **1b** (a) and **1c** (b).

Linear DNA can be generated from supercoiled pUC18 DNA by double strand breaks, single strand breaks or a mixture of double strand and single strand breaks. The cleavage pattern exhibited by our compounds points to mainly a single strand scission process since most of Form I is converted into Form II. But, interestingly, the formation of linear DNA (Form III) long before disappearance of supercoiled DNA (Form I) (lanes 4-11 and 10-14, Figure 7a and 7b, respectively) implies that a double strand cleavage pathway plays a role as well.[35] This is of

some significance from a practical standpoint inasmuch as double-stranded DNA cleavage cannot be repaired intracellularly; therefore **1b** and **1c** can be considered as potential drug candidates.

DNA photocleavage mechanism

It is well-known that DNA photocleavage mediated by a photosensitizer (PS) occurs through a mechanism in which the photosensitizer, initially at ground state (PS^0), is irradiated at the appropriate wavelength and then passes to a short-lived singlet excited state ($^1PS^*$) that may convert to a long-lived triplet state ($^3PS^*$) (Scheme 2). This triplet state is the photoactive one which may generate reactive oxygen species through two main mechanisms, named as type I and type II. Type I reactions involve an electron or a hydrogen transfer that leads to the formation of superoxide and hydroxyl radicals. In type II reactions, there is an energy transfer from the photocleaver triplet state to O_2, that mediates the formation of singlet oxygen ($^1O_2$), which is able to oxidize nucleobases, especially guanine.[2a, 3a, 34]

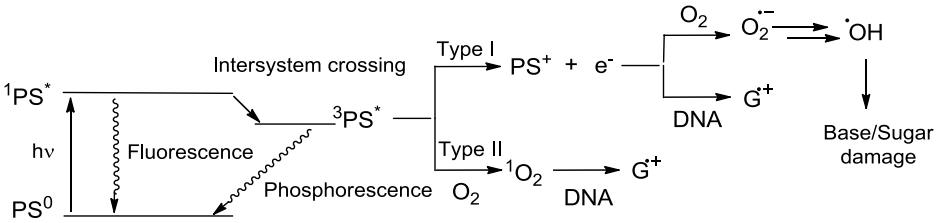

Scheme 2. General DNA photocleavage mechanism.

To gain better insight in the photocleavage process mediated by compounds **1b** and **1c** and in order to elucidate the cleavage pathway we performed some mechanism investigations. The involvement of reactive oxygen species (ROS) such as singlet oxygen, superoxide and hydroxyl radicals in the nuclease mechanism was determined by monitoring the quenching of the DNA photocleavage in the presence of ROS scavengers. To clarify other mechanistic aspects, groove binders such as Hoescht (minor groove binder) or methyl green (major groove binder) were also used. Results are shown in Figure 9. Quantitative data are collected in Tables S3 and S4.

The addition of standard radical hydroxyl scavengers (sodium formate and DMSO) attenuated significantly the DNA cleavage promoted by **1b** (lanes 3 and 5, Figure 9a) indicating that freely diffusible hydroxyl radicals are involved in the DNA scission process. In the case of compound **1c,** sodium formate (lane 3, Figure 9b) and DMSO (lane 5, Figure 9b) cause only a slight cleavage inhibition. KI blocked the DNA photocleave promoted by both compounds (lanes 4, Figure 9a and 9b). However, this result should not be only attributed to the participation of hydroxyl radicals in the cleavage reaction but also to KI ability to quench **1b** and **1c** fluorescence emission, an effect that was observed once KI was added to the reaction mixture.The important involvement of singlet oxygen ($^1O_2$) in the DNA photocleavage mechanisms of both compounds was evidenced by the significant increase of cleavage in the presence of D_2O (lanes 2, Figures 9a and 9b). For compound **1b** a complete DNA degradation (smearing) was observed. In the case of compound **1c** supercoiled DNA in the presence of D_2O yielded to Form II and Form III. Singlet oxygen scavengers (TMP, DABCO and NaN_3) (lanes 6-8, Figure 9a) also confirmed the relevant role of $^1O_2$ in the photocleavage process mediated by **1b**. DNA strand scission is attenuated in the presence of these radical scavengers, and consequently a significant increase of supercoiled DNA (Form I) and a decrease of open circular DNA (Form II) were observed. The inhibitory effect of these singlet oxygen scavengers on DNA cleavage mediated by **1c** was much lower (lanes 6-8, Figure 9b). DNA photocleavage was blocked in the presence of Tiron, which clearly indicates the participation of $O_2^{\bullet-}$ in the DNA breakdown promoted by both triazolopyridopyrimidines (lane 13 for **1b** and lane 11 for **1c**).

All these results enable us to deduce that **1b** and **1c** DNA photocleavage occurs by an oxidative pathway involving mainly singlet oxygen but also superoxide and hydroxyl radicals. Therefore, the scission process takes place through both type I and type II mechanisms.

The minor effect of radical scavengers observed in the photo-induced DNA cleavage mediated by **1c** could be explained considering the minor ability of this compound to produce these reactive oxygen species. Morever, the lack of DNA damage observed for **1a** could be, at least in part, due to a decrease in singlet oxygen production simply upon its direct binding to DNA in a similar way to that described for several photosensitizers.[3c]

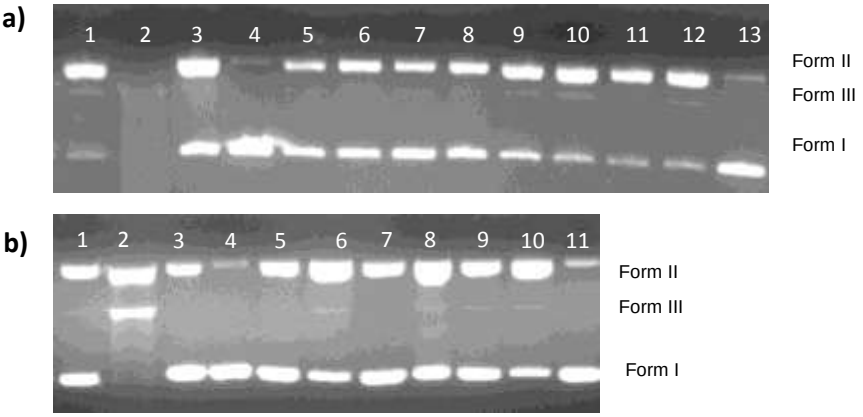

Figure 9. a) Agarose gel electrophoresis of pUC18 of 80 μM compound **1b** upon photo-irradiation at 365 nm for 2 h. 1: **1b** 80 μM; 2: **1b** + D_2O; 3: **1b** + Sodium formate 0.4 M; 4: **1b** + KI 0.4 M; 5: **1b** + DMSO 0.4 M; 6: **1b** + 2,2,6,6-tetramethyl-4-piperidone (TMP) 0.4 M; 7: **1b** + 1,4-diazabicycle [2,2,2] octane (DABCO) 0.4 M; 8: **1b** + NaN_3 0.4 M; 9: **1b** + Methyl green 3 μM; 10: **1b** + Methyl green 6 μM; 11: **1b** + Hoescht 8 μM; 12: **1b** + Hoescht 16 μM; 13: **1b** + Tiron 10 mM. **b)** Agarose gel electrophoresis of pUC18 of 90 μM compound **1c** upon photo-irradiation at 365 nm for 2 h. 1: **1c** 90 μM; 2: **1c** + D_2O; 3: **1c** + Sodium formate 0.4 M; 4: **1c** + KI 0.4 M; 5: **1c** + DMSO 0.4 M; 6: **1c** + 2,2,6,6-tetramethyl-4-piperidone (TMP) 0.4 M; 7: **1c** + 1,4-diazabicycle [2,2,2] octane (DABCO) 0.4 M; 8: **1c** + NaN_3 0.4 M; 9: **1c** + Methyl green 6 μM; 10: **1c** + Hoescht 16 μM; 11: **1c** + Tiron 10 mM.

The addition of neither major groove binder methyl green (lanes 9 and 10 for **1b** and lane 9 for **1c**) nor minor groove binder Hoescht 33258 (lanes 11 and 12 for **1b** and lane 10 for **1c**) produced significant changes in DNA photocleavage induced by both compounds. This result is in good agreement with those derived from binding studies that revealed no DNA interaction with **1b** or **1c**. Therefore, it can be deduced that **1b** and **1c** promote DNA photocleavage generating diffusible radicals and without an appreciable DNA interaction.

A similar result has been reported for a Ru(II) complex, $[Ru(bipy)_3]^{2+}$, a photosensitizer that only weakly associates with DNA but that is able to cause oxidative DNA damage through ROS in the presence of light.[36] More recently, light activation of DNA binding has been reported for several transition metal complexes through excited states[37] however, to our knowledge, this phenomenon has not been described for small organic molecules. This fact encouraged us to study a possible interaction of photo-activated compounds **1b** and **1c** with DNA.

Within this context, thermal denaturation assays were performed on samples containing CT-DNA and the corresponding compound after photo-exposure to UVA light during 2 hours (Figure S7). In these experiments, no significant changes in CT-DNA melting temperature were observed which suggests that compounds **1b** and **1c** are not able to photo-bind DNA.

At this stage, we thought about the possibility that irradiation of triazolopyridopyrimidines **1** could generate an intermediate species that directly could be related to their photonuclease

activity. In this sense, the study of electrochemical and photochemical properties of compounds **1a**, **1b** and **1c** after photoexcitation may shed some light on this regard.

First, we analyzed the cyclic voltammograms of compounds **1a**, **1b** and **1c** upon light irradiation (λ_{max}= 365 nm) during 2 hours. Compounds **1a** and **1c** presented the same voltammogram as without photoirradiation. However, a new cathodic peak at E_{pa}= -0.87 V was found in the voltammogram of **1b**, which indicates the presence of a new species in solution as a result of **1b** photoactivation (Figure S8).

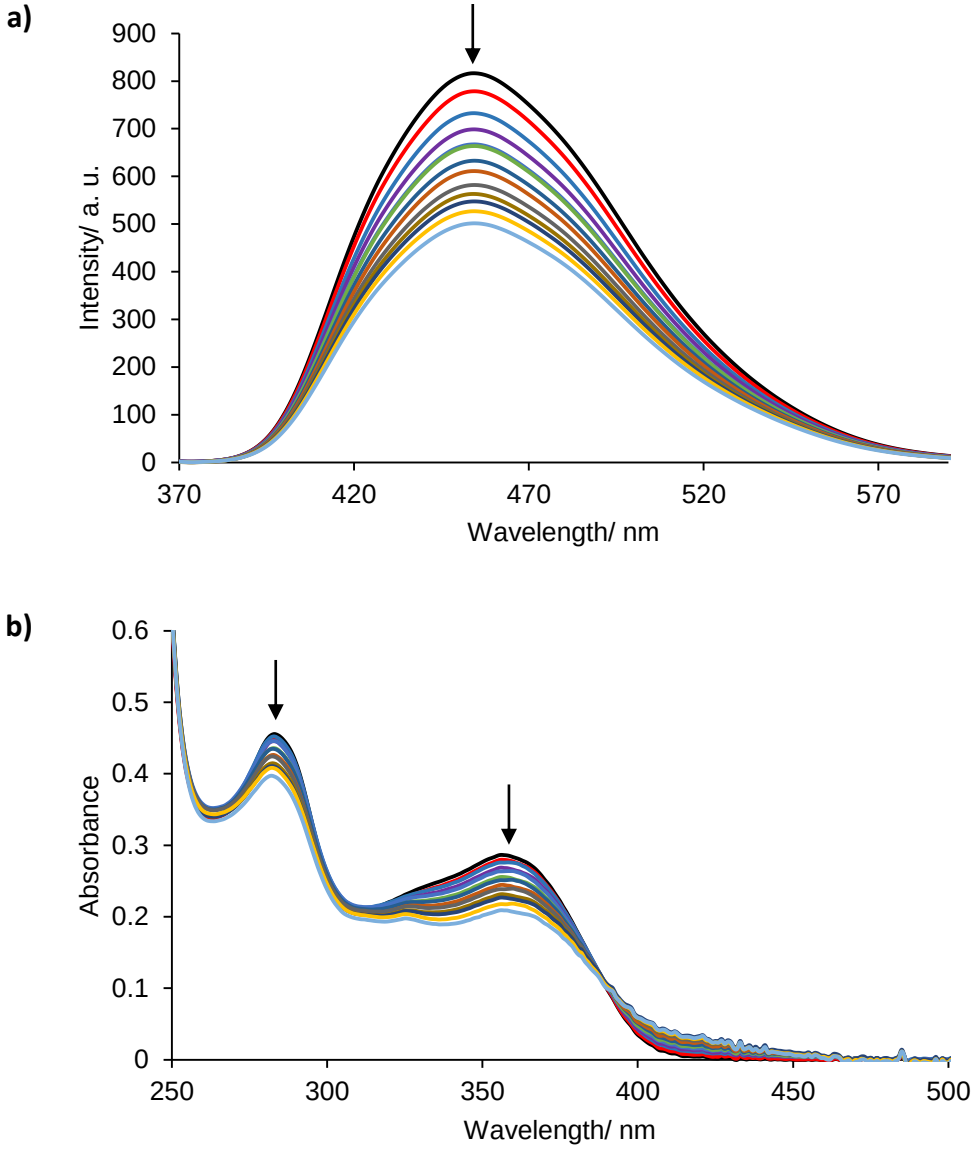

Figure 10. a) Fluorescence emission spectra **1b** in cacodylate buffer 0.1 M, pH= 6.0, 5% DMF upon irradiation (λ_{max}= 365 nm) each 10 minutes until 2 h. **b)** UV absorbance spectra of **1b** in cacodylate buffer 0.1 M, pH= 6.0, 5% DMF, after irradiation (λ_{max}= 365 nm) each 10 minutes up to 2 h. Arrows indicate the effect of irradiation in UV absorbance and fluorescence emission.

Also, we performed a series of experiences in which the absorbance in UV-visible and the fluorescent emission of a solution of each compound after UVA irradiation were monitored. Samples were irradiated up to 2 hours and the spectra were recorded at intervals of 10 minutes. Noteworthy, fluorescence and UV spectra of **1b** display significant changes upon

photoexcitation (Figure 10). By contrast, fluorescence and UV spectra of compounds **1a** and **1c** do not undergo significant modifications upon irradiation. In particular, the UV spectrum of compound **1b** exhibits a remarkable hypochromism and an isosbestic point at 391 nm that suggest one step equilibrium of two stable species in solution. As a tentative, this finding could mean that irradiation of **1b** yields to a triazolopyridopyrimidine derivative which could be responsible, at least in part, for the higher DNA photocleavage efficiency of **1b** compound. Attempts to detect this derivative species through ^{1}H NMR were unsuccessful

With all these results, a plausible mechanistic pathway for the DNA photocleavage reaction mediated by compounds **1b** and **1c** could be postulated (Scheme 3). In this proposed pathway, on the basis of previous studies on triazolopyridines,[38] an equilibrium between the corresponding triazolopyridopyrimidine **1** and its diazo open form (**1-diazo**) has been firstly considered. UV-A irradiation initiates the primary photochemical processes that lead to electronically excited states (**1*** and/or **1-diazo***). The excited states can return to their ground states undergoing two major competing reactions: electron transfer (type I pathway) or energy transfer (type II pathway). The type I mechanism gives rise to superoxide that forms hydroxyl radicals. At the same time, from the excited states (**1*** and/or **1-diazo***) energy is transferred to triplet oxygen that it is converted into singlet oxygen. Finally, the reactive oxygen species generated ($^1O_2$, superoxide and hydroxyl radicals) produce DNA damage.

This proposed pathway can also explain the difference in photocleavage activity of our triazolopyridopyrimidine compounds. The higher DNA cleavage activity of **1b** could be attributed to its major ability for generate ROS that, ultimately, may be related to diazo form concentration. In fact, DFT calculations for triazolopyridines[38] have shown that the triazol-diazo equilibrium lies more to the right for unsubstituted triazol derivatives than for 3-methyl substituted triazol compounds.

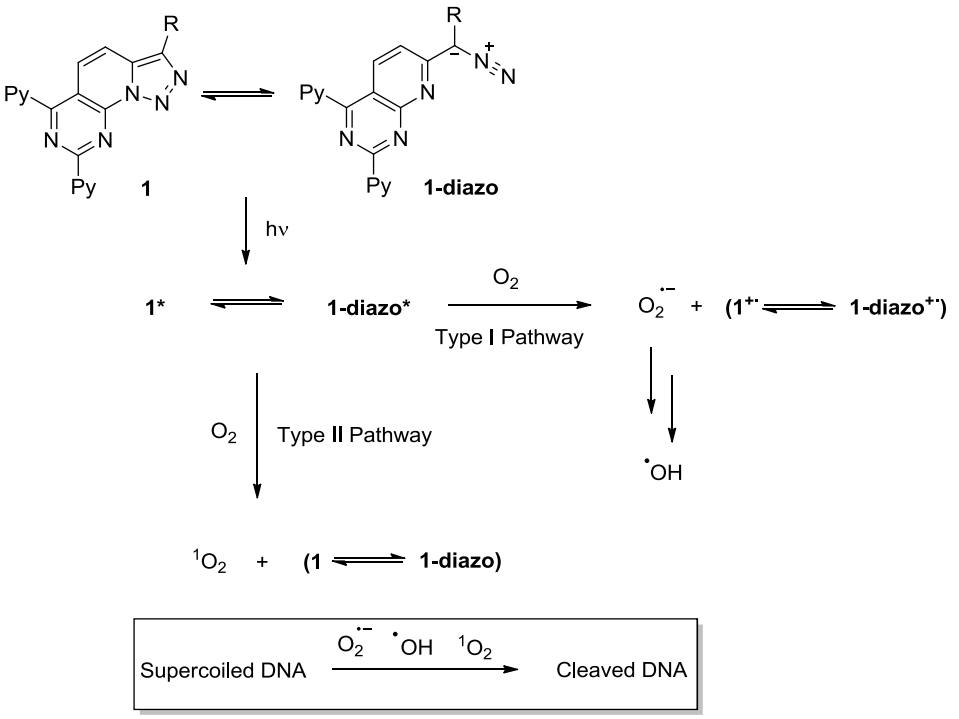

Scheme 3. Proposed mechanism of DNA photocleavage mediated by compounds **1b** and **1c**.

Antileishmanial activity

Leishmaniasis is considered to be within the most relevant group of neglected tropical diseases, affecting millions of people worldwide. It is caused by several species of protozoa

belonging to the family Trypanosomatidae and genus *Leishmania*. Current treatment of the disease is based on chemotherapy. However, it is far from being satisfactory because most of the drugs are toxic or expensive.[39]

Some of the currently used drugs for the treatment of leishmaniasis, such as pentamidine[13] or furamidine[14], act at DNA level. Furthermore, we have recently described a series of triazolopyridyl ketone derivatives able to interact with DNA and with remarkable antileishmanial activities.[12] In this context, and due to the structural relation between triazolopyridopyrimidines and triazolopyridyl ketones, the antileishmanial activity of compounds **1a-c** was evaluated.

In vitro activity against *Leishmania spp*

Firstly, compounds **1a-c** were tested for their antiprotozoal activity against promastigotes of four different *Leishmania* species (*L. infantum*, *L. braziliensis*, *L. guyanensis* and *L. amazonensis*), as well as for cytotoxicity against J774 macrophages. As it can be inferred from data presented in Table 3, compound **1b** was no active while compounds **1a** and **1c** resulted active at micromolar level and did not present toxicity. These results seem to suggest that the substitution at C3 position of the triazol ring enhance the antileishmanial activity of triazolopyridopyrimidines. Noteworthy, compound **1a** showed to be more active than the reference antileishmanial agent, miltefosine, against the four *Leishmania spp*. This compound also presented very high selectivity index (SI = CC_{50}/IC_{50}) and, therefore, it could be considered as a promising therapeutic agent.

Table 3. Leishmanicidal activities of triazolopyridopyrimidines **1** on extracellular forms (*Leishmania* promastigotes) and cytotoxicity on J774 macrophages.

Comp.	Parasites IC_{50}[a] (μM)								Cell lines CC_{50}[b](μM)
	L. inf	SI[c]	*L. amaz*	SI	*L. braz*	SI	*L. guy*	SI	Macrophages J774
1a	9.71	30.89	13.53	22.71	19.08	15.72	9.19	32.64	NC[e]
1b	NA[f]		NA[f]		NA[f]		NA[f]		NC
1c	73.56	3.38	42.69	5.84	57.55	4.33	48.12	5.18	NC
M[d]	21.3	7.7	28.3	5.8	27.1	6.0	53.6	3.1	163.6

[a]IC_{50}, concentration of the compound that produced a 50% reduction in parasites; [b]CC_{50}, concentration of the compound that produced a 50% reduction of cell viability in treated culture cells with respect to untreated ones; [c]Selectivity Index = CC_{50}/IC_{50}; [d]M, miltefosine; [e]NC= non cytotoxic, $CC_{50} \geq 300$ μM; [f]NA, non-active at tested concentrations.

The next step was to test the two active compounds, **1a** and **1c**, against *L. amazonensis* and *L. infantum* intracellular amastigotes (Table 4), as these are the clinically relevant forms of the parasite.

Table 4. *In vitro* activity of triazolopyridopyrimidines **1a** and **1c** on *L. infantum* and *L. amazonensis*, intracellular forms (amastigotes).

Compound	Intracellular amastigotes			
	L. infantum		*L. amazonensis*	
	IC_{50}[a](μM)	SI[b]	IC_{50} (μM)	SI
1a	19.54	15.35	114.58	2.61
1c	13.68	21.92	71.24	4.21

M[c]	23.7	5.7	20.9	6.5

[a]IC_{50}, concentration of the compound that produced a 50% reduction in parasites; [b]SI = CC_{50}/IC_{50}; [c]M, miltefosine.

In the case of *L. amazonensis* amastigotes, the antileishmanial activity of both compounds was lower than the one of miltefosine. However, in the assay against *L. infantum* amastigotes compounds **1a** and **1c** resulted to be more active and selective than miltefosine.

In a certain way, the high activity of compound **1a** could be associated to its demonstrated propensity for DNA binding but, taking into account results of compound **1c,** other different mechanism contributing to the activity of the triazolopyridopyrimidines should be considered.

In vivo activity against *Leishmania infantum*

The good results against *L. infantum* amastigotes for compounds **1a** and **1c** encouraged us to test their *in vivo* activity against the same *Leismania* species in a murine model of acute infection. The compounds were assayed at concentrations of 5 mg/kg, administered daily by the intraperitoneal route up to a total of 5 doses, using a method previously described.[40] Results are shown in Table 5.

Although compound **1c** resulted totally inactive, compound **1a** exhibited high leishmanicidal activity against spleen forms. This finding suggests that compound **1a,** represents a possible candidate for drug development in the therapeutic control of leishmaniasis.

Table 5. *In vivo* antileishmanial effect of **1a** and **1c** against *L. Infantum.*

Compound	Percentage Reduction[a] (Mean ± SD[b])	
	Spleen	Liver
1a	84.93 ±21.73*	NS[c]
1c	NS[c]	NS[c]

[a]Reduction of parasite burden in spleens and livers of treated mice in relation to those in the control (untreated) groups expressed as percentage; [b]standard deviation (SD) was calculated by comparing individual data for each treated animal with the mean value for the control group; [c]NS: Not suppression in parasite burden; *$p < 0.05$.

Conclusions

The main objective of this work was to investigate the ability of a series of triazolopyridopyrimidines (**1a-c**) to bind to DNA and to act as DNA photocleavers for Photodynamic Therapy (PDT). Moreover, the leismanicidal activity of compounds **1a-c** was tested.

DNA binding studies with both genomic duplex DNA and synthetic sequences have revealed that **1b** and **1c** are not able to interact with DNA while compound **1a** presents high DNA affinity and exhibits some preference for the GC.CG step sequence. The interaction of **1a** at DNA grooves seems to be driven by hydrophobic interactions in which the phenyl moiety plays a key role. Moreover, the fluorescence quenching of **1a** in the presence of DNA together with its potential values suggest that photooxidation processes, which involve mainly guanine, take place upon binding of **1a** to DNA.

Interestingly, triazolopyridopyrimidines **1b** and **1c** have been shown to be efficient DNA photocleavage agents. Mechanistic investigations on the DNA damage process have shown that both **1b** and **1c** act through a type II pathway associated to singlet oxygen formation and through a type I pathway leading to superoxide and hydroxyl radicals generation. The higher DNA photocleavage activity of **1b** could be attributed to its major ability for generate ROS that, ultimately, may be related to its higher propensity for triazol ring opening reaction to yield the corresponding open diazo form.

On the other hand, compounds **1a** and **1c** display significant *in vitro* activity against *L. infantum* amastigotes, the clinically relevant forms of the parasite. Furthermore, *in vivo* tests revealed that compound **1a** presented high leishmanicidal activity against spleen forms of the same species.

In summary, in this work we have evidenced that triazolopyridopyrimidines are a novel structural class of 1,2,3-triazoles with interesting properties *versus* DNA. Clearly, our results have indicated that the nature of the substituent at C3 position of triazolopyridopyrimidines strongly determines their DNA binding capacity and/or their DNA photocleavage activity. In particular, compound **1b** has demonstrated to be a very attractive candidate for DNA photocleavage with potential applications in Photodynamic Theraphy (PDT).

Experimental Section

Synthesis

Materials and methods. Melting points were determined on a Büchi B-545. NMR spectra were recorded on a Bruker AC300MHz or 500MHz in $CDCl_3$ or DMSO-d_6 as solvent. COSY experiments were done for all compounds. HRMS Electron Impact (EI) or ElectroSpray (ES) determinations were made using a VG Autospec Trio 1000 (Fisons). UV-vis spectra were performed with Agilent 8453 UV-vis spectrophotometer. Fluorescence spectra were recorded on a a JASCO FP-6200 spectrofluorimeter. All the lithiation reactions were done under inert atmosphere and dry solvents.[41] All reagents were pursached from Aldrich.

*Synthesis of **1b** and **1c.*** 6,8-Di(pyridin-2-yl)-[1,2,3]triazolo[1',5':1,6]pyrido[2,3-*d*]pyrimidine (**1b**) and 3-methyl-6,8-di(2-pyridyl)-[1,2,3]triazolo[5',1':6,1]pyrido[2,3-*d*]pyrimidine (**1c**) were prepared as described elsewhere.[15a, b]

*Synthesis of 3-phenyl-6,8-di(2-pyridyl)-[1,2,3]triazolo[5',1':6,1]pyrido[2,3-d]pyrimidine **(1a)*** To a solution of 3-phenyl-[1,2,3]triazolo[1,5-*a*]pyridine[42] (3 g, 15.3 mmol) in anhydrous toluene at –40 ºC, 1.1 equivalents of *n*-BuLi in hexane (1.5 M, 11.2 mL) were added with stirring. A deep red colour developed. The mixture was kept at –40 ºC (30 min). Treatment with a dry toluene solution (10 mL) of 2.1 equivalents of 2-cyanopyridine (3.3 g, 32.1 mmol) produced a colour change to yellow. The reaction mixture was left at room temperature during 2 hours and then quenched with 15 mL of a 10% HCl solution. After 1 hour of stirring it was neutralized with NaOH(aq). Then, the organic layer was separated and the aqueous layer extracted with dichloromethane. The organic layers were joined and dried over anhydrous Na_2SO_4. Evaporation of the organic solvents gave place to a residue which was purified by alumina (IV) chromatography, eluting with hexane/AcOEt. Firstly, 3-phenyl-[1,2,3]triazolo[1,5-a]pyridin-7-yl pyridin-2-yl methanone[15a] was eluted (596 mg, 13%). When polarity was increased a yellow solid identified as 3-phenyl-6,8-di(2-pyridyl)-[1,2,3]triazolo[5',1':6,1]pyrido[2,3-d]pyrimidine **1a** (2.2 g, 36%) was obtained. m.p. 252-255 ºC (AcOEt); ^{1}H NMR (300 MHz, $CDCl_3$, 25 ºC, TMS): δ= 7.60 - 7.42 (m, 5H), 8.06 - 7.92 (m, 5H), 8.62 (ddd, *J* = 8.0, 1.1, 1.1Hz, 1H), 8.87 (ddd, *J* = 4.8, 1.8, 0.9Hz, 1H), 8.90 (d, *J* = 9.7Hz, 1H), 8.93 (ddd, *J* = 8.0, 1.1, 1.1Hz, 1H), 8.96 (ddd, *J* = 4.7, 1.8, 0.9Hz, 1H); ^{13}C NMR (75 MHz, $CDCl_3$, 25°C, TMS): δ= 163.6 (C), 161.7 (C), 155.5 (C), 153.7 (C), 150.4 (CH), 149.5 (C), 148.9 (C), 140.9 (C), 137.6 (CH), 137.1 (CH), 130.5 (CH), 130.3 (C), 129.1 (CH), 128.6 (CH), 127.2 (CH), 126.0 (CH), 125.6 (CH), 125.2 (CH), 125.0 (CH), 124.6 (CH), 117.6 (CH), 113.5 (C); UV/Vis: λ_{max} (cacodylate buffer 0.1 M (pH=6.0), 5% DMF)/nm 280 (ε/ dm^3

$mol^{-1}cm^{-1}$ 16218), 387 (8912); Fluorescence emission: λ_{max} (cacodylate buffer 0.1 M (pH=6.0), 5% DMF)/nm, λ_{exc}= 286, 376; λ_{em}= 519; HRMS (EI): Calculated mass for $C_{24}H_{15}N_7$: 401.1389, Found mass: 401.1378. EM (I.E): *m/z* (%): 373 (100), 295 (6).

DNA interaction studies

DNA solution preparation. Stock CT-DNA (Type XV, Sigma-Aldrich) and poly(dG-dC)$_2$ (Sigma-Aldrich) solutions were prepared in distillated water, while that of poly(dA-dT)$_2$ (Sigma-Aldrich) was prepared in cacodylate buffer 0.1 M, (pH= 6.0) and 10 mM NaCl. DNA concentration in nucleotides was determined by the UV absorbance at 260 nm for CT-DNA, 262 nm for poly(dA-dT)$_2$ and 254 nm for poly(dG-dC)$_2$ after 1:20 dilution using the known molar extinction coefficients of each polynucleotide:[43] $\varepsilon_{CT\text{-}DNA}$ = 6600 M^{-1} cm^{-1}, $\varepsilon_{poly(dA\text{-}dT)2}$= 6600 M^{-1} cm^{-1} and $\varepsilon_{poly(dG\text{-}dC)2}$= 8400 M^{-1} cm^{-1}.

Electronic absorption titrations. The UV-Vis spectrum of the samples were recorded at 25 ºC on a Agilent 8453 UV-vis spectrophotometer equipped with a Peltier temperature-controlled sample cell and driver (Agilent 89090A). Electronic absorption titrations were performed by adding increasing amounts of CT-DNA to a solution of the assayed compound at a fixed concentration. Samples were prepared in cacodylate buffer 0.1 M (pH=6.0), 5% DMF. After each addition of CT-DNA, the mixtures were allowed to equilibrate before the spectra were recorded. To correct the absorbance of DNA itself, the UV spectra of CT-DNA alone were recorded at the same experimental conditions and then, DNA spectra were substracted from the spectra of the DNA + compound.

Fluorescence titrations. The fluorescence spectra were recorded on a JASCO FP-6200 spectrofluorimeter at room temperature. Fluorescence titrations experiments were performed by adding increasing amounts of DNA (CT-DNA, poly(dA-dT)$_2$ or poly(dG-dC)$_2$) to a solution of the tested compound at a fixed concentration. Samples with a final volume of 3 mL were prepared in cacodylate buffer 0.1 M (pH =6.0), 5% DMF.

[$K_4Fe(CN)_6$] titrations. These experiences were carried out following the same methodology described above for UV titrations on JASCO FP-6200 spectrofluorimeter. $K_4[Fe(CN)_6]$ solutions were prepared fresh daily in distillated deoxygenated water. Titrations were performed by adding increasing concentrations of $K_4[Fe(CN)_6]$ (final concentrations ranging from 0.15 μM to 3 μM) to a solution of 1a (15 μM) or 1a (15 μM) and CT-DNA (90 μM) in cacodylate buffer 0.1 M (pH= 6.0), 5% DMF. After each $K_4[Fe(CN)_6]$ addition the mixtures were equilibrated for 5 minutes prior to their fluorescence emission spectra were recorded.

Viscosity measurements. Viscosity experiments were carried out with a semi-micro Ubbelodhe viscosimeter immersed in a Julabo ME16G thermostated bath maintained at 25.0 ± 0.1 ^{o}C. Samples (4 mL) contained the assayed compound (with final concentrations ranging from 1-15 μM) and calf thymus DNA (50 μM) in cacodylate buffer 0.1 M (pH = 6.0), 5 % DMF. Flow times were measured in triplicate with a stopwatch. Data were presented as $(\eta/\eta_0)^{1/3}$ *vs.* the ratio of the compound concentration to DNA, where η is the viscosity of DNA in the presence of the compound and η_0 is the viscosity of DNA alone. Viscosity values were calculated from the observed flow time of a solution containing DNA corrected for the flow time of buffer alone (t_0), $\eta = t - t_0$.

Cyclic Voltammetry. Cyclic voltammetry experiments were performed in a single compartment cell with a three-electrode system on a PAR 273A potentiostat/galvanostat. The working and auxiliary electrode were platinum, and the reference electrode was Ag/AgCl. The supporting electrolyte was tetrabutylammonium perchlorate. Solutions of the compounds (2.5 mM) in DMF were deoxygenated by purging with nitrogen for 15 min prior to measurement.

DNA photocleavage

The photoinduced cleavage of pUC18 DNA by the compounds was studied by agarose gel electrophoresis. A stock solution of the compound to be tested was prepared in DMF. 2 μL of this solution were used for individual reactions. Samples were prepared by mixing 17.5 μL of 0.1 M cacodylate buffer (pH 6.0), 0.5 μL of pUC18 (0.25 μg/μL) (Thermo Scientific), 2 μL of a solution of compound at increasing concentrations to obtain final concentrations between 5 μM and 18 μM (compound **1a**) or between 25 μM and 100 μM (compounds **1b** and **1c**). DNA control samples were prepared by mixing 17.5 μL of 0.1 M cacodylate buffer (pH 6.0), 2 μL of DMF and 0.5 μL of pUC18 (0.25 μg/μL). Reactions were carried out under illuminated conditions using UVA lamps (λ_{max}= 365 nm) (Luzchem Research, Inc.). Samples in eppendorf vials were photo-exposed for 2 h, those that were not photoirradiated were maintained at 37 ºC in the darkness. In the case of compound **1a** samples were incubated for 1 h at 37 ºC in dark conditions before light exposure. After that, 4 μl of electrophoresis loading buffer (0.25% bromophenol blue, 0.25% xylene cyanol dye, 30% glycerol) were added to the samples that finally were loaded on a 0.8% agarose gel in 0.5 x TBE buffer (0.045 M tris, 0.045 M boric acid, and 1 mM EDTA) containing 2 μL/100 mL of a solution of ethidium bromide (10 mg/ mL). The electrophoresis was carried out in dark at 80 V for 2 h. The bands were visualized with UV light and photographed on a capturing gel printer plus TDI.

The relative amounts of supercoiled, open circular and linear DNA forms were quantified by densitometry analysis using the ImageJ 1.34s software.[44] A correction factor of 1.3 was used for the assessment of supercoiled DNA (Form I) since the intercalation between EB and Form I DNA is relatively weak compared with that of Form II (nicked) and Form III (linear) DNA.[45]

DNA photocleavage mechanism

To test the presence of reactive oxygen species (ROS) generated during light induced DNA scission, various reactive oxygen intermediate scavengers were added to the reaction mixtures prior to light exposure. The scavengers used were 2,2,6,6-tetramethyl-4-piperidone (0.4 M), 1,4-diazabicyclo[2,2,2]octane (DABCO) (0.4 M), 4,5-dihydroxy-1,3-bencenesulphonic acid (Tiron) (10 mM), sodium formate (0.4 M), potassium iodide (0.4 M), DMSO (0.4 M), sodium azide (0.4M). For the D_2O experiment, this solvent was used for dilution of the sample solution to a volume of 20 μl. To test possible compound-DNA interactions sites the major groove binder methyl green (3 or 6 μM) and the minor groove binder Hoescht 33258 (8 or 16 μM) were also assayed. Samples were treated as described above.

Leishmanicidal activity

Drugs and reagents. Resazurin sodium salt and Miltefosine were obtained from Sigma-Aldrich. Resazurin sodium salt was stored at 4 ^{o}C protected from light. The solution of resazurin was prepared at 2.5 mM in phosphate buffered saline solution (PBS), pH 7.4, and filtered through 0.22 μm prior use.

Parasites and culture procedure. The following species of *Leishmania* were used: an autochthonous isolate of *L. infantum* (MCAN/ES/96/BCN150) obtained from an asymptomatic dog from the Priorat region (Catalunya, Spain), kindly given by Prof. Montserrat Portús (Universidad de Barcelona); *L. braziliensis* 2903, *L. amazonensis* (MHOM/Br/79/Maria) and *L. guyanensis* 141/93 were kindly provided by Prof. Alfredo Toraño (Instituto de Salud Carlos III, Madrid). Promastigotes were cultured in Schneider's Insect Medium (Sigma) at 26 ^{o}C supplemented with 20% heat-inactivated Foetal Bovine Serum (FBS) (Sigma) and 100 U/mL of penicillin plus 100 μg/mL of streptomycin (Sigma) in 25 mL culture flasks.

In vitro promastigote susceptibility assay. This assay was performed following a method previously described.[40] Briefly, log-phase promastigotes (2.5 × 10^5parasites/well) were cultured in 96-well plastic plates. Compounds were dissolved in dimethylsulfoxide (DMSO) and were added at 2-fold serial dilutions up to 200 μL final volume. The final solvent (DMSO) concentrations never exceeded 0.2% (v/v). After 48 h at 26 ^{o}C, 20 μL of 2.5 mM resazurin

solution was added and the fluorescence intensity (535 nm-excitation wavelenght- and 590 nm-emission wavelenght-) was determined with a spectrofluorimeter Infinite 200 (Tecan i-Control) to calculate growth inhibition (%). All tests were carried out in triplicate. Miltefosine was used as reference drug. The efficacy of each compound was estimated by calculating the IC_{50} (concentration of the compound that produced a 50% reduction in parasites).

In vitro intracellular amastigote susceptibility assay. Assays were carried out as described by Bilbao-Ramos et al.[46] Briefly, 5×10^4 J774 macrophages and stationary promastigotes in a 1:10 rate were seeded in each well of a microtiter plate, suspended in 200 µL of culture medium and incubated for 24 h at 33 ^oC, 5% CO_2 in humidity chamber. After this first incubation, the temperature was increased up to 37 ^oC for another 24 h. Thereafter, cells were washed several times in culture medium by centrifugation at 1.500 g for 5 min in order to remove free non-infective promastigotes. Finally, the supernatant was replaced by 200 µL/well of culture medium containing 2-fold serial dilutions of the test compounds in a triplicate assay. Following incubation for 48h at 37 ^oC, 5% CO_2 in humidity chamber, the culture medium was replaced by 200 µL/well of the lysis solution (RPMI-1640 with 0.048% HEPES and 0.006% SDS) and incubated at room temperature for 20 min. Thereafter, the plates were centrifuged at 1,500g for 5 min and the lysis solution was replaced by 200 µL/well of Schneider´s insect medium. The culture plates were then incubated at 26 ^oC for other 3 days to allow transformation of viable amastigotes into promastigotes and proliferation. Afterwards, 20 µL/well of 2.5 mM resazurin was added and left for another 3h incubation. Finally, fluorescence emission was measured as described above.

In vivo leishmanicidal assay. The *in vivo* assay was performed in BALB/c mice infected with the virulent *L. infantum* strain MCAN/ES/96/BCN150. The infection was carried out in the same conditions as previously described.[40] Briefly, each mouse was infected with 10^7 promastigotes at stationary phase, given by the intracardiac (IC) route following anaesthesia with sodium pentobarbital. The splenic and hepatic parasite burden were estimated by the limiting dilution assay described by Titus et al.[47] adapted to the conditions of our laboratory.The therapeutic protocols were carried out as follows: Mice were randomly sorted into seven groups. One group was kept as untreated control. Treatment started on the twenty-one day post-infection and lasted for 5 continuous days. Animals were dosed once daily and the compounds were administered at 5 mg/kg given by the intraperitoneal route in a 0.1 mL final volume of propylene glycol solution. Seven days later, the mice were sacrificed and the parasitic burden was evaluated.

All animal experiments and procedures were approved by the institution´s committee on the ethical handling and protection of laboratory animals used for experimental and other scientific purposes.

Cytotoxicity assays

Cell cultures. J774 murine macrophages were grown in RPMI 1640 medium (Sigma) supplemented with 10% heat-inactivated Fetal Bovine Serum, FBS (30 min at 56 ^oC), penicillin G (100 U/mL) and streptomycin (100 µg/mL). For the experiments, cells in the pre-confluence phase were harvested with trypsin. Cell cultures were maintained at 37 ^oC in a humidified environment with 5% CO_2.

Cytotoxicity assays on macrophages J774. The procedure for cell viability measurement was evaluated with resazurin by a colorimetric method described previously.[48] Macrophages. J774 cell lines were seeded (5×10^4 cells/well) in 96-well flat-bottom microplates with 100 µL of RPMI 1640 medium. The cells were allowed to attach for 24h at 37 ^oC, 5% CO_2 and the medium was replaced by different concentrations of the drugs in 200 µL of medium, and exposed for another 24h. Growth controls were also included. Afterwards, 20 µL of the 2.5 mM resazurin solution was added and plates were returned to incubator for another 3h to evaluate cell viability. The reduction of resazurin was determined by the fluorescence intensity (535 nm-excitation wavelenght- and 590 nm-emission wavelenght) as in the promastigotes assay. Each

concentration was assayed three times. Medium and drug controls were used in each test as blanks.

Statistics. Data are reported as means of three repeated experiments. The efficacy against parasite (IC_{50}) and the cytotoxicity effect (CC_{50}) of compounds were determined by probit multilineal analysis curves. For *in vitro* test all data were analyzed by Tukey's HSD-test post-hoc and *in vivo* assays were analyzed by U-Mann Whitney. Statistical significance was considered at $p \leq 0.05$ using SPSS v20.0 and Microsoft Excel 2007 software.

Acknowledgments

We are grateful to the Ministerio de Ciencia e Innovación (Spain) (Project CONSOLIDER-INGENIO SUPRAMED CSD 2010-00065), to Generalitat Valenciana (Valencia, Spain) (Project PROMETEO 2011/008) for their financial support. The authors thank SCSIE (University of Valencia) for the assistance with HRMS. R.A. acknowledges Generalitat Valenciana for a doctoral fellowship.

References

[1] K. Groger, D. Baretic, I. Piantanida, M. Marjanovic, M. Kralj, M. Grabar, S. Tomic and C. Schmuck, *Org. Biomol. Chem.* **2011**, *9*, 198-209.
[2] a) C. J. Burrows and J. G. Muller, *Chem. Rev.* **1998**, *98*, 1109-1152; b) W. K. Pogozelski and T. D. Tullius, *Chem. Rev.* **1998**, *98*, 1089-1108; c) J. A. Cowan, *Curr. Opin. Chem. Biol.* **2001**, *5*, 634-642; d) F. Mancin, P. Scrimin, P. Tecilla and U. Tonellato, *Chem. Commun.* **2005**, 2540-2548.
[3] a) Y. N. Konan, R. Gurny and E. Allémann, *J. Photo. Photobiol. B Biol.* **2002**, *66*, 89-106; b) R. Bonnett, *J. Heterocycl. Chem.* **2002**, *39*, 455-470; c) J. F. Lovell, T. W. B. Liu, J. Chen and G. Zheng, *Chem. Rev.* **2010**, *110*, 2839-2857; d) M. Ethirajan, Y. Chen, P. Joshi and R. K. Pandey, *Chem. Soc. Rev.* **2011**, *40*, 340-362; e) S. L. H. Higgins and K. J. Brewer, *Angew. Chem. Int. Ed.* **2012**, *51*, 11420-11422.
[4] X. Li, Y. Lin, Q. Wang, Y. Yuan, H. Zhang and X. Qian, *Eur. J. Med. Chem.* **2011**, *46*, 1274-1279.
[5] a) T. Aravinda, N. H. S. Bhojya and N. H. R. Prakash, *Int. J. Pept. Res. Ther.* **2009**, *15*, 273-279; b) S.-F. Cui, Y. Ren, S.-L. Zhang, X.-M. Peng, G. L. V. Damu, R.-X. Geng and C.-H. Zhou, *Bioorg. Med. Chem. Lett.* **2013**, *23*, 3267-3272.
[6] a) K. Lemke, M. Wojciechowski, W. Laine, H. Bailly, P. Colson, M. Baginski, A. K. Larsen and A. Skladanowski, *Nucleic Acids Res.* **2005**, *33*, 6034-6047; b) E. Zabost, A. M. Nowicka, Z. Mazerska and Z. Stojek, *Phys. Chem. Chem. Phys.* **2012**, *14*, 3408-3413.
[7] W. M. Cholody, S. Martelli and J. Konopa, *J. Med. Chem.* **1990**, *33*, 2852-2856.
[8] J. Węsierska-Gądek, N. Zulehner, F. Ferk, A. Składanowski, O. Komina and M. Maurer, *Biochem. Pharmacol.* **2012**, *84*, 1318-1331.
[9] H. Kusnierczyk, W. M. Cholody, J. Paradziej-ˇˇLukowicz, C. Radzikowski and J. Konopa, *Arch. Inmunol. Ther. Exp* **1994**, *42*, 415-423.
[10] E. Augustin, A. Moś-Rompa, A. Skwarska, J. M. Witkowski and J. Konopa, *Biochem. Phamacol.* **2006**, *72*, 1668-1679.
[11] a) E. L. da Silva Jr., R. F. S. Menna-Barreto, M. d. C. F. V. Pinto, R. S. F. Silva, D. V. Teixeira, M. C. B. V. de Souza, C. A. De Simone, S. L. De Castro, V. F. Ferreira and A. V. Pinto, *Eur. J. Med. Chem.* **2008**, *43*, 1774-1780; b) V. Patil, W. Guerrant, P. C. Chen, B. Gryder, D. B. Benicewicz, S. I. Khan, B. L. Tekwani and A. K. Oyelere, *Bioorg. Med. Chem.* **2010**, *18*, 415-425; c) A. Tahghighi, S. Razmi, M. Mahdavi, P. Foroumadi, S. K. Ardestani, S. Emami, F. Kobarfard, S. Dastmalchi, A. Shafiee and A. Foroumadi, *Eur. J. Med. Chem.* **2012**, *50*, 124-128.
[12] R. Adam, P. Bilbao-Ramos, S. López-Molina, B. Abarca, R. Ballesteros, M. E. González-Rosende, M. A. Dea-Ayuela and G. Alzuet-Piña, *Bioorg. Med. Chem.* **2014**, *22*, 4018-4027.

[13] P. G. Bray, M. P. Barrett, S. A. Ward and H. P. de Koning, *Trends Parasitol.* **2003**, *19*, 232-239.
[14] E. M. de Souza, A. Lansiaux, C. Bailly, W. D. Wilson, Q. Hu, D. W. Boykin, M. M. Batista, T. C. Araújo-Jorge and M. N. C. Soeiro, *Biochem. Pharmacol.* **2004**, *68*, 593-600.
[15] a) B. Abarca, R. Ballesteros and M. Chadlaoui, *ARKIVOC* **2002**, *(x)*, 52-60; b) B. Abarca, R. Aucejo, R. Ballesteros, M. Chadlaoui, E. Garcia-Espana and C. Ramirez de Arellano, *ARKIVOC* **2005**, *(xiv)*, 71-75; c) M. Chadlaoui, B. Abarca, R. Ballesteros, C. Ramirez de Arellano, J. Aguilar, R. Aucejo and E. Garcia-Espana, *J. Org. Chem.* **2006**, *71*, 9030-9034.
[16] H. He, P.-C. Lo and D. K. P. Ng, *Chem. Eur. J.* **2014**, *20*, 6241-6245.
[17] M. Tian, H. Ihmels and E. Brotz, *Dalton Trans.* **2010**, *39*, 8195-8202.
[18] J. A. Cowan, *Inorganic Biochemistry: An Introduction*, VHC Publishers Inc, USA, **1993**, p.
[19] P. Mpountoukas, A. Pantazaki, E. Kostareli, P. Christodoulou, D. Kareli, S. Poliliou, C. Mourelatos, V. Lambropoulou and T. Lialiaris, *Food Chem. Toxicol.* **2010**, *48*, 2934-2944.
[20] M. Sirajuddin, S. Ali and A. Badshah, *J. Photochem. Photobiol. B Biol.* **2013**, *124*, 1-19.
[21] P. Živec, F. Perdih, I. Turel, G. Giester and G. Psomas, *J. Inorg. Biochem.* **2012**, *117*, 35-47.
[22] A. Wolfe, G. H. Shimer and T. Meehan, *Biochemistry* **1987**, *26*, 6392-6396.
[23] X. Li, Y. Lin, Y. Yuan, K. Liu and X. Qian, *Tetrahedron* **2011**, *67*, 2299-2304.
[24] J. B. Lepecq and C. Paoletti, *J. Mol. Biol.* **1967**, *27*, 87-106.
[25] J. B. Chaires, N. Dattagupta and D. M. Crothers, *Biochemistry* **1982**, *21*, 3933-3940.
[26] T. W. Plumbridge and J. R. Brown, *Biochem. Pharmacol.* **1978**, *27*, 1881-1882.
[27] T. Phillips, I. Haq, A. J. H. M. Meijer, H. Adams, I. Soutar, L. Swanson, M. J. Sykes and J. A. Thomas, *Biochemistry* **2004**, *43*, 13657-13665.
[28] a) C. Moucheron, A. Kirsch-De Mesmaeker and J. M. Kelly, *J. Photo. Photobiol. B Biol.* **1997**, *40*, 91-106; b) A. Ghosh, P. Das, M. R. Gill, P. Kar, M. G. Walker, J. A. Thomas and A. Das, *Chem. Eur. J.* **2011**, *17*, 2089-2098.
[29] C. A. M. Seidel, A. Schulz and M. H. M. Sauer, *J. Phys. Chem.* **1996**, *100*, 5541-5553.
[30] X.-L. Zhao, Z.-S. Li, Z.-B. Zheng, A.-G. Zhang and K.-Z. Wang, *Dalton Trans.* **2013**, *42*, 5764-5777.
[31] S. J. Burya, D. A. Lutterman and C. Turro, *Chem. Commun.* **2011**, *47*, 1848-1850.
[32] J. Liu, T. Zhang, T. Lu, L. Qu, H. Zhou, Q. Zhang and L. Ji, *J. Inor. Biochem.* **2002**, *91*, 269-276.
[33] L. E. Joyce, J. D. Aguirre, A. M. Angeles-Boza, A. Chouai, P. K. L. Fu, K. R. Dunbar and C. Turro, *Inorg. Chem.* **2010**, *49*, 5371-5376.
[34] B. Armitage, *Chem. Rev.* **1998**, *98*, 1171-1200.
[35] J.-T. Wang, Q. Xia, X.-H. Zheng, H.-Y. Chen, H. Chao, Z.-W. Mao and L.-N. Ji, *Dalton Trans.* **2010**, *39*, 2128-2136.
[36] C. V. Kumar, J. K. Barton and N. J. Turro, *J. Am. Chem. Soc* **1985**, *107*, 5518-5523.
[37] S. L. H. Higgins, A. J. Tucker, B. S. J. Winkel and K. J. Brewer, *Chem. Commun.* **2012**, *48*, 67-69.
[38] F. Blanco, I. Alkorta, J. Elguero, V. Cruz, B. Abarca and R. Ballesteros, *Tetrahedron* **2008**, *64*, 11150-11158.
[39] a) M. P. Barrett and S. L. Croft, *British Med. Bull.* **2012**, *104*, 175-196; b) K. Chauhan, M. Sharma, R. Shivahare, U. Debnath, S. Gupta, Y. S. Prabhakar and P. M. S. Chauhan, *ACS Med. Chem. Lett.* **2013**, *4*, 1108-1113.
[40] M. A. Dea-Ayuela, E. Castillo, M. Gonzalez-Alvarez, C. Vega, M. Rolón, F. Bolás-Fernández, J. Borrás and M. E. González-Rosende, *Bioorg. Med. Chem.* **2009**, *17*, 7449-7456.
[41] D. Perrin and L. F. Armarego, *Purification of Laboratory Chemicals, 3rd Ed.*, Pergamon, Oxford, **1988**, p.
[42] J. H. Boyer, R. Borgers and L. T. Wolford, *J. Am. Chem. Soc.* **1957**, *79*, 678-680.
[43] K. R. Fox in *Drug-DNA interaction protocols, Vol. 90* Humana Press Inc, New Yersey, **1997**, p. 223.
[44] W. Rasband in *Image J 1.34s, Vol.* National Institutes of Health, USA.
[45] R. P. Hertzberg and P. B. Dervan, *J. Am. Chem. Soc* **1982**, *104*, 313-315.

[46] P. Bilbao-Ramos, S. Sifontes-Rodríguez, M. A. Dea-Ayuela and F. Bolás-Fernández, *J. Microbiol. Methods* **2012**, *89*, 8-11.
[47] R. G. Titus, M. Marchand, T. Boon and J. A. Louis, *Parasite Inmunol.* **1985**, *7*, 545-555.
[48] M. Rolón, E. M. Seco, C. Vega, J. J. Nogal, J. A. Escario, A. Gómez-Barrio and F. Malpartida, *Int. J. Antimicrob. Agents* **2006**, *28*, 104-109.